

Nanofabrication of electrodes with sub-5 nm spacing for transport experiments on single molecules and metal clusters

A. Bezryadin^{a)} and C. Dekker

Department of Applied Physics and DIMES, Delft University of Technology, Lorentzweg 1, 2628 CJ Delft, The Netherlands

(Received 20 March 1997; accepted 16 May 1997)

Electron-beam deposition is used to fabricate free-standing carbon nanoelectrodes separated by a gap of less than 5 nm. Fabrication is carried out under direct visual control in an electron microscope. After coating the carbon electrodes with a thin metal film (e.g., AuPd) such structures can be used to study electrical transport properties of single molecules (e.g., conjugated polymers) or metal nanoclusters. The fabrication process of the nanowires is described in detail. Furthermore, we suggest electrostatic trapping as a new method to bridge the electrodes with a single conducting nanoparticle in a controlled way. This principle was tested successfully on Pd nanoclusters and carbon nanotubes. © 1997 American Vacuum Society. [S0734-211X(97)13704-0]

I. INTRODUCTION

There has been much speculation about the prospect of "molecular electronics," i.e., electronic devices with single molecules as the active elements.¹ This may provide an attractive direction for the future development of electronic devices for several reasons. It conceptually can give the highest possible degree of circuit integration, viz., devices at the atomic scale. Devices may also operate at extremely high frequencies. Since different combinations of atoms give an almost infinite variety of chemical properties of resulting molecules, as is obvious from chemistry, one may expect that molecules with desired electronic properties can be synthesized as well. Many examples of molecules with an electronic functionality have already been synthesized, e.g., quantum wires such as conjugated polymers, molecular switches, molecular rectifiers, etc.^{1,2} Direct dc measurements of electrical properties of single molecules are lacking however. Usually experiments probe the conducting properties of a macroscopic amount of molecules. Here, hopping of electrons between molecules dominates transport. As a consequence, the intramolecular charge transport has not been well studied. This strongly contrasts the interesting theoretical predictions for electron transport through single molecular chains.³ Direct measurements of transport through single molecules will allow the verification of this, and are prerequisite for an assessment of the feasibility of molecular-scale electronics. Such experiments constitute the motivation for the technical developments of nanoelectrodes and electrostatic trapping reported in this article. The new techniques presented here may enable transport studies on single molecules.

There are two major problems which have to be solved to enable electrical transport experiments on single molecules. First, it is necessary to prepare conducting electrodes separated by a distance which at most equals the length of the molecule which has to be measured. This presents a difficulty because the available molecules of interest are usually

much smaller than the resolution limits (~ 10 – 20 nm) of the conventional electron beam lithography.⁴ For example, rigid conjugated oligomers of well-defined length are usually up to about 5 nm in length.⁵ Second, one has to find a way to bridge those electrodes with a single molecule. In this article we present a solution to both two obstacles.

Our method of fabrication of small gaps takes advantage of the electron beam deposition (EBD) of amorphous carbon which can be achieved in a scanning electron microscope (SEM).⁶ The SEM provides direct visual control which is an important advantage with respect to standard lithography. With EBD we can grow two free-standing carbon wires towards each other and adjust the gap between them to be as small as 3 nm. This is sufficiently small to bridge the electrodes by available conjugated oligomers.⁵

The principle of EBD is known since the pioneer work of Broers and co-workers.^{4,6} If the electron beam in a SEM is focused at a spot, it locally decomposes organic contamination molecules which usually are present in a small amount at the sample surface. It can, for example, be an ultrathin film of the pump oil due to a bad vacuum of the system. The decomposition of organic material leads to the deposition of a rigid⁷ solid material which is a mixture of amorphous carbon and some polymers.⁸ As soon as the contamination molecules in the e-beam spot are transformed into amorphous carbon, new organic material diffuses from other parts of the sample surface to the top of the carbon hill. The growth process thus proceeds continuously in time. As a result, by fixing the e-beam at a spot, a vertical carbon needle with a high aspect ratio can be deposited.⁸ By scanning the beam it is possible to locally cover the sample with carbon, which subsequently can be used as a protecting mask during an etching procedure. This method is known as contamination lithography⁶ which has a high resolution of about 10 nm.

Deposition of individual molecules or metal nanoclusters between two metallic electrodes is an issue which is being pursued by many research groups.^{9–11} In order to bridge the electrodes with a single conducting molecule or a metal cluster we suggest a new method, viz., electrostatic trapping

^{a)}Electronic mail: bezryadi@qt.tn.tudelft.nl

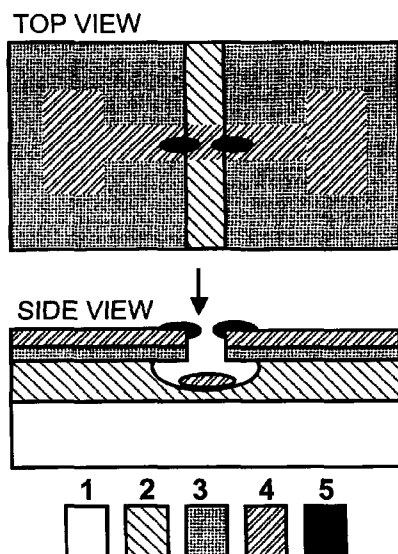


FIG. 1. Schematic view of the sample. It includes (1) a Si wafer, (2) a $1\text{ }\mu\text{m}$ thick SiO_2 film, (3) a low stress 60 nm thick film SiN, (4) a 10 nm thick AuPd film with contact pads, and (5) electron beam deposited carbon electrodes separated by a small gap, possibly less than 5 nm . The arrow shows the orientation of the electron beam during the growth of carbon nanoelectrodes. A metal film (not shown) is sputtered on top of the free-standing carbon electrodes to improve their conductivity.

(ET). This is a universal technique which can be used with any type of conducting particle. The principle is the following. Suppose we have two closely spaced electrodes which are immersed in a dilute solution of molecules or nanoclusters in some nonconducting solvent. If now a voltage of, say, 1 V is applied to the electrodes, then a very strong electric field, 10^8 V/m for a gap of 10 nm , will appear. Note that the electric field will exhibit a strong gradient, falling off quickly outside the gap. This field will polarize conducting nanoparticles in the neighborhood of the gap. The polarized particles will be attracted to the point of the strongest field, i.e., to the region right between the electrodes. The positively charged side of the molecule is attracted to the negative electrode and the negative side to the positive electrode. The electrodes thus will be connected by the molecule if the distance between them is sufficiently small.

Below we discuss the sample layout developed for experiments on single molecules (Sec. II), then we reiterate the principle of EBD and present details of fabrication of the free-standing carbon wires interrupted by a nanogap (Sec. III). Metal coating of these is presented in Sec. IV. Finally, we present some first results of electrostatic trapping of Pd nanoparticles and carbon nanotubes (Sec. V).

II. SAMPLE LAYOUT FOR TRANSPORT EXPERIMENTS ON SINGLE NANOPARTICLES

The sample layout is shown in Fig. 1. The sample consists of a silicon wafer covered with a film of SiO_2 and a thin low-stress SiN film. A narrow slit is etched in the SiN film in

SF_6 plasma. In the next step we slightly underetch the SiN film in HF acid to form an undercut. Due to this undercut, a thin AuPd film sputtered across the slit has an interruption of the order of 100 nm in width. Within this gap we grow two amorphous carbon needles towards each other. The needles are grown in a SEM using the electron beam deposition technique. An advantage of this layout is that the electrodes are free-standing, so one can evaporate metal on them (to improve their conductivity or to reduce the spacing between them) without making a short cut. The leakage resistance between the gold contact pads is very high, about $10^{13}\text{ }\Omega$ due to the thick SiO_2 layer. Another advantage is the possibility to image trapped particles with SEM, or—after a slight modification such as etching a hole through the Si wafer—with transmission electron microscopy (TEM).

The fabrication steps are as follows. We start with a Si wafer covered with a $1\text{ }\mu\text{m}$ thick thermally grown siliconoxide layer, and a 60 nm thick ultralow-stress SiN film made by low-pressure chemical-vapor deposition.¹² The next step is the etching of a long slit in the SiN film. Before etching, a 300 nm film of poly(methylmethacrylate) (PMMA) (950 K) resist is spun at 5000 rpm onto the sample to protect the SiN film. Patterning of the resist is carried out in an electron beam pattern generator. The slit usually is about $100\text{--}150\text{ nm}$ in width and a few mm in length. After the slit is made by means of reactive ion etching in a SF_6 plasma, we slightly underetch the underlying SiO_2 with HF acid. The etching rate of SiN in 40% HF solution is 4 nm/min ; SiO_2 is etched at a rate of about 1500 nm/min . Underetching during about 20 s results in a free-standing SiN membrane of approximately 500 nm in width divided into two parts by the slit as it is shown in Fig. 1. Next we sputter across the slit a strip of gold or gold palladium of $10\text{--}20\text{ nm}$ in thickness and about $20\text{ }\mu\text{m}$ in width. For the pattern definition of the strip a mechanical shadow mask (not shown) is used. The mask is made from a Si wafer (100) by anisotropic etching in KOH. The slit cuts the gold strip into two parts separated by the 100 nm gap. It is inside this gap that we grow the carbon nanowires starting from the edges of the gold film. Due to the underlying SiO_2 layer the leakage resistance between the Au electrodes is about $10^{13}\text{ }\Omega$ while the total area of Au electrodes including the contact pads is a few square millimeters. The high value of the leakage resistance is important, because it acts as a parallel resistance to that of the single nanoparticle which is localized between the carbon electrodes during the measurements. And we will see below, a single particle can have a rather low conductivity.^{13,14}

III. ELECTRON BEAM DEPOSITION OF FREE-STANDING CARBON NANOWIRES

The last two steps of the fabrication process are the growth of two carbon nanowires towards each other and coating them with a thin metal film to improve their conductivity. These issues will be described in details in this and the next section, respectively. As indicated in Fig. 1, the nanowires are attached to the gold electrodes with the underlying SiN membrane and stay within the plane of the membrane.

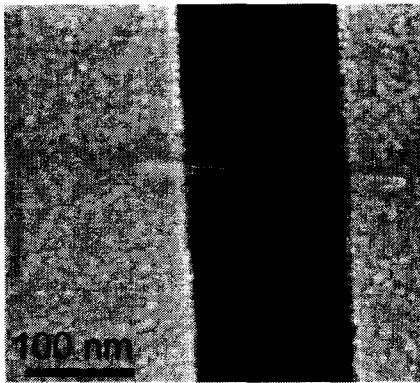


FIG. 2. A free-standing amorphous carbon wire of about 10 nm in width, grown by a slow linear scan of the electron beam across the slit in the SiN membrane. The electron beam deposition was done after sputtering of a 20 nm thick AuPd film on the membrane. The metal film makes electrical connection to the carbon wire and provides a convenient amount of organic contamination which is necessary for the EBD. The electron beam scan rate was about 3 nm/s.

The growth process should be stopped when the desired distance between their tips is achieved. We have succeeded in making this distance as small as 3 nm. The low limit is determined by the resolution of SEM (about 1 nm for our Hitachi S-900 SEM) and the growth rate which is between 1 and 10 nm/s in our case. The latter can be reduced if necessary by cleaning the sample in oxygen plasma or stopped by cooling to 77 K.

In practice, free-standing horizontal carbon nanowires are fabricated in the following way. We focus the beam on the gold film near the edge of the membrane and then move it slowly (~ 1 nm/s) towards the slit. Initially the deposition occurs at the gold film but as soon as the beam leaves the membrane a free-standing carbon needle starts to grow parallel to the membrane, inside the slit. If the e-beam sweep rate is too high, i.e., higher than the deposition rate, the needle cannot follow the beam and the growth process is interrupted. If on the other hand the e-beam velocity is too slow, a sheet of carbon rather than a rod is formed with a large size in the direction of the beam, which is much higher than the width in the direction perpendicular to the beam and to the motion. To grow a thin symmetric carbon rod we start scanning the beam with a high velocity across the slit periodically, and then slowly decrease the beam velocity until the growing carbon wire can follow the beam. The width of electron beam deposited needles usually is between 5 and 20 nm (see for example, Fig. 2). If necessary it can be reduced down to about 3 nm by a slow etching in an oxygen plasma. The electron beam deposited carbon is poorly electrically conducting, especially at low temperatures. Consequently carbon nanowires can be used as a template for the fabrication of narrow one-dimensional metal wires, or more sophisticated patterns by simply depositing a metal film on top.¹⁵

An alternative way of making free-standing structures takes advantage of the feedback control of the signal of secondary electrons.¹⁵ In this case the beam is positioned *in* the

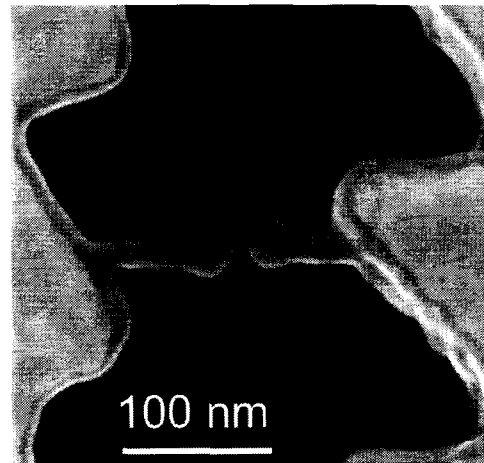


FIG. 3. Two free-standing carbon nanowires grown towards each other using the electron beam deposition technique. They are separated by a distance of about 4 nm. Gold grains visible behind the whiskers are not in focus because they are lying about $0.5 \mu\text{m}$ below the nanowires, on the bottom of the groove (see the sample layout in Fig. 1). The small value of the gap is achieved by zooming in the SEM on the area around the gap. This results in a thickening of the tips of the electrodes. The acceleration voltage and the e-beam current were 30 kV and about 20 pA correspondingly.

slit, close (~ 5 nm) to the membrane edge. Initially the signal of secondary electrons is zero because the beam does not cross anything. The deposition of carbon starts on the membrane regardless of the fact that the beam does not touch it.¹⁶ After some time (~ 10 s) the carbon needle reaches the e-beam and some secondary-electron signal appears. When the signal reaches a certain level, we step the beam away from the membrane edge and wait again till the needle reaches the beam. This procedure is carried out repeatedly. Of course such an algorithm can also be applied to a continuously moving beam. The feedback process usually results in somewhat thicker rods than the linear scan method.

Now let us see how a gap of a few nm can be achieved. Of course one can grow two whiskers towards each other from the opposite sides of the slit. But it is difficult to make a small, say < 5 nm, gap from the very beginning, because it is not possible to observe the first nanowire while growing the second one, since the beam does not scan the area for imaging but moves along with the second carbon wire. However, an initial gap of, say, 30 nm can easily be made in this way. Then to reduce the gap it is sufficient to zoom in the SEM on the nanowires near the gap, i.e., the tips of both carbon needles should be visible on the SEM screen. During the ordinary imaging the process of continuous deposition of carbon slowly proceeds at all points of the area that is scanned by the electron beam. Consequently the nanorods grow in size and the gap between them decreases continuously. When the distance between their tips reaches desired value, the SEM is switched off. The smallest gap we did fabricate by this method was less than 3 nm. An example is shown in Fig. 3. Note that the amorphous carbon nanowires are very rigid and chemically inert, so the gap is very stable.

It does for instance not change when the sample is cleaned with different solvents or acids.

As we have seen, EBD is a powerful technique for nanofabrication. It provides the possibility of fabricating structures of nm dimensions under direct visual control. It does not require resist and, accordingly, EBD is not limited to fabrication of structures on a planar surface. It gives a possibility to grow free-standing nanostructures. A possible drawback is the use of a surface contamination as a precursor which commonly is supposed to arise from the bad vacuum. This may render the process not well-reproducible because the contamination depends on the cleanliness of the SEM machine. The level of the contamination in our Hitachi SEM is very low. Therefore the deposition is very slow or it does not occur at all if the sample has been cleaned by an oxygen plasma or through a wet etch in aqua regia ($\text{HNO}_3:\text{HCl}$, 1:3).

We have optimized the technique for better reproducibility by investigating cleaning procedures and well-characterized precursor materials. We have tried various organic liquids as precursors. The liquid should wet the surface to form a thin uniform film and it should not be too volatile in order to have it stay on the surface when the sample is exposed to the vacuum inside the SEM. It was found that liquid paraffin (a mixture of hydrocarbons from $\text{C}_{12}\text{H}_{26}$ to $\text{C}_{18}\text{H}_{38}$) gives a very high deposition rate of about 100 nm/s or higher. To form a thin paraffin film on the surface the sample can be immersed in a solution of the paraffin in cyclohexane (1:100) and then dried in a flow of nitrogen gas. It is a good precursor but the EBD rate is very high. Hexadecane ($\text{C}_{16}\text{H}_{34}$) turned out to be a more suitable precursor for our applications. This organic liquid wets our sample surface and can be decomposed by the electron beam. The presence of traces of this slightly volatile liquid on the surface provides a convenient EBD rate (from 1 to 10 nm/s). To cover the sample with this liquid precursor it is sufficient to put a drop of $\text{C}_{16}\text{H}_{34}$ on the surface and then dry the sample in a nitrogen flow during a few seconds. A convenient way to contaminate the surface and enable EBD is to sputter a thin metal film. In this case the contamination is due to the bad vacuum in the sputtering machine. In both cases ($\text{C}_{16}\text{H}_{34}$ precursor or sputtering contamination) EBD occurs in a very similar way and results in carbon wires of similar sizes and quality. EBD occurs also in the TEM under the influence of the parallel, very broad beam of electrons. By cooling the sample down to the liquid nitrogen temperature it is possible to stop the deposition process and image the sample without modifying the amorphous carbon nanostructures.

IV. METAL COATING OF THE CARBON ELECTRODES

The resistivity of EBD amorphous carbon usually is quite high (10^2 to $10^5 \Omega \text{ cm}$ at room temperature) and rather irreproducible. For transport experiments one needs electrodes with a sufficiently high and predictable conductivity. This can be achieved by coating the carbon needles with an amorphous or small-grain-size metal film, by sputtering or evaporation. If the experiment has to be done in air the coating

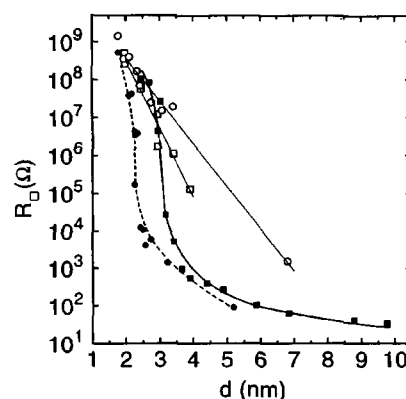


FIG. 4. Square resistance R_{\square} vs film thickness, d , for various sputtered thin films. Solid squares represent AuPd (4:1) films on SiN. Solid circles denote AuPd films on a very thin (0.3 nm) sticking layer of chromium which serves to suppress the granularity. Here R_{\square} is shown vs the total thickness of AuPd and Cr film. Open symbols show the square resistance of films which are sputtered onto carbon wires grown by EBD.

material should not oxidize. Also the metal film should not be thick, otherwise it will reduce or even close the gap between the electrodes. We have investigated the efficiency of the gold palladium (4:1) as a coating material. The square resistance of films sputtered on a smooth dielectric surface (SiO_2 or SiN) is plotted versus the film thickness in Fig. 4 (solid squares). The resistance starts to rise very sharply,¹⁷ even on this log scale, when the thickness becomes lower than 3 nm. SEM imaging shows that below this value the film consists of isolated grains. The granularity can be reduced if one first sputters a few Å of Cr. In this case, even a 2.5 nm film has already a quite low resistance, $R_{\square} \sim 10^4 \Omega$ (Fig. 4, solid circles). Note that after sputtering of the Cr film, the sample was exposed to air for about 1 min before the subsequent sputtering of AuPd was carried out.

A qualitatively different behavior of the film resistance versus thickness is found when the film is sputtered onto the carbon wires such as shown in Fig. 2. The resistance of such films drops exponentially with decreasing thickness, which is slower than for films on a planar substrate. The difference is probably due to the fact that in two dimensions (on the planar substrate) a percolation path appears at some critical size of the grains. This leads to the jumpwise drop of the square resistance. The metal film on a carbon nanowire is effectively one-dimensional because the metal-grain size is of the same order of magnitude as the wire diameter. Therefore there is only one possible path, and it is improbable that all grains on this path are touching each other. Now if there is at least one interruption, then electrons have to tunnel across it (probably through the carbon substrate). The size of interruptions will probably be inversely proportional to the film thickness. The resistance then is an exponential function of the film thickness. The current-voltage characteristics (not shown) of all ultrathin coating films are linear.

The metal coating technique also provides an alternative way of making small gaps. In Fig. 5 we present two nan-

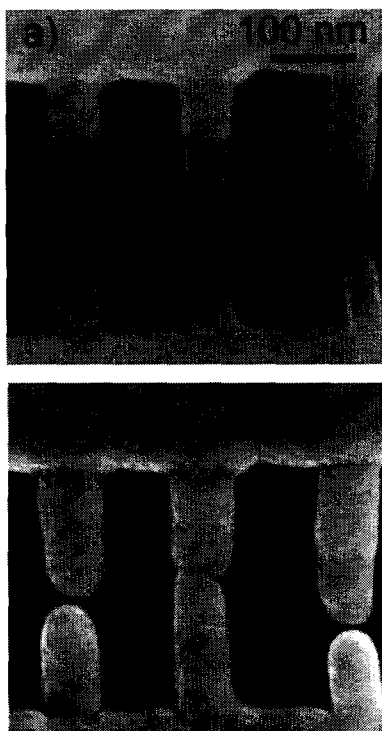


Fig. 5. Free-standing carbon nanowires (bright in the pictures) (a) before and (b) after coating with a thin AuPd film. The coating reduces the spacing between the electrodes by approximately 11 nm (from 16 to 5 nm). Note that this is a factor of 3 smaller than the sputtered film thickness which is about 30 nm in the present case.

ogaps between carbon needles, before and after coating with a 30 nm film of AuPd. By choosing the appropriate size of the initial gap and the AuPd film thickness, it is possible to reduce the gap down to 5 nm by coating, as shown in Fig. 5. Note that right after the coating the sample was cleaned in oxygen plasma (50 W) for about 5 min. In independent tests we have verified that such cleaning does not etch the AuPd electrodes. The cleaning is necessary to remove organic contamination to enable the high-resolution imaging without depositing a new layer of carbon. It was also found that the oxygen plasma etches away the underlying carbon so one can obtain free-standing gold palladium wires.

We thus have demonstrated two ways of making electrodes separated by a very small (<5 nm) distance. In the first technique, a nanogap of *desirable* size is fabricated by EBD under visual control in SEM. Then electrodes are coated with a few nm (say 4 nm) thin film to improve their conductivity. The gap reduction caused by the coating is small, about 1–2 nm in this case, because, as shown in Fig. 5, the gap reduction is smaller than the sputtered film thickness by a factor of ~ 3 . The second possibility is to start with a quite large (e.g., 20 nm) initial gap and then sputter sufficient metal to reduce the gap size to the desired value. The smooth coating [Fig. 5(b)] makes this process quite reproducible, but nevertheless a few steps of sputtering usually are

necessary before the desired small gap size will be achieved. Let us mention also a third possibility, which has not been verified in our study. By using organometallic compounds as precursor material one can grow needles which consist of metallic nanograins surrounded by amorphous carbon.¹⁸ This may yield a rather low resistivity ($0.01 \Omega \text{ cm}$). This implies a carbon electrode resistance of $\sim 10 \text{ k}\Omega$ (without coating) which is sufficiently low for molecular transport experiments.

V. ELECTROSTATIC TRAPPING OF SINGLE CONDUCTING NANOPARTICLES

Suppose we have two electrodes with a spacing smaller than the length of a molecule or a metal cluster. Then, a single nanoparticle may be fixed between the electrodes by means of ET. The principle of ET is the following. First we apply a voltage to the electrodes thus creating a strong electric field in the gap. If a conducting nanoparticle comes close to the gap it will be polarized by the electric field near the gap. Then, like any dipole, it will be oriented along the field, and will be attracted to the region of the strongest field, i.e., to the gap between electrodes. The positive side of the polarized molecule will be attracted to the negative electrode and the negative side to the positive. The molecule thus will bridge the electrodes. This principle of electrostatic trapping is expected to work for any type of conducting nanoparticles, i.e., molecules with delocalized electrons, metallic clusters, carbon nanotubes, etc.

To bring the molecules close to the electrodes one by one, one can immerse the electrodes in a dilute solution of molecules. Another possibility would be to expose the electrodes to a vapor of molecules in an ambient inert gas. Molecules will diffuse and from time to time come close to the gap. Here they will be trapped electrostatically as explained above. As soon as one molecule is trapped, a current will flow between the electrodes, and the sample can be withdrawn from the solution or vapor. Clearly, a good solvent for ET should not conduct electrically, so there is no current between the electrodes before a molecule is trapped. Also it should not be polar, since this would lead to screening of the field in the gap.

It is interesting to note that if one applies a series resistor R_s between the voltage source and electrodes, with a value much higher than the resistance of the molecule R_m , then the electrostatic field in the gap will be strongly reduced (by a factor R_s/R_m) as soon as one molecule is trapped. As a consequence, trapping of a second particle may be prevented.

We have tested ET on carbon nanotubes and palladium colloid particles. These have been chosen because of their relatively big size which provides the possibility to image them with SEM and directly verify the efficiency of the ET. Carbon nanotubes are long cylindrical molecules containing only carbon atoms.¹⁹ Single-wall nanotubes were synthesized by Smalley and co-workers.²⁰ They are not solvable in any known solvent but can be ultrasonically dispersed in various organic liquids. We have used cyclohexane where a small amount of soot containing the nanotubes was dispersed

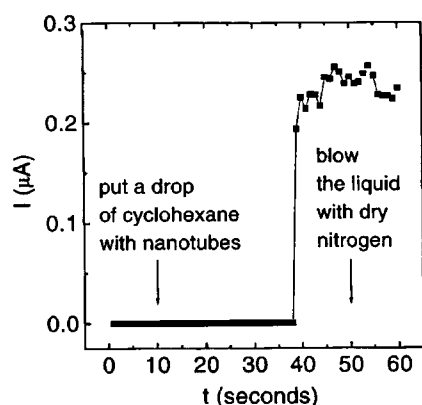


FIG. 6. Variation of the current flowing between the electrodes during a trapping experiment. The voltage was fixed at 4.5 V; the series resistor was 10 M Ω . The distance between the electrodes was about 150 nm.

ultrasonically. After excitation during a few minutes the soot was not visible any more and the suspension was transparent. It contains single nanotubes, bundles of parallel nanotubes ("ropes"²⁰), tangles of ropes, and pieces of amorphous carbon. Therefore only a part of the trapping experiments resulted in a single rope lying across the electrodes.

Trapping events can be detected by measuring the current between the electrodes in real time. During ET the current usually changes as shown in Fig. 6. In this experiment we applied 4.5 V to the electrodes through a series resistor of 10 M Ω . Then we put a drop of the nanotube dispersion in cyclohexane on the electrodes at $t = 10$ s. After about 30 s a finite current was detected which indicates that a nanotube rope is trapped on the electrodes. Upon drying the liquid at $t = 50$ s the current did not change. In some cases a considerable reduction (about one order of magnitude) of the resistance was observed during the drying. Examples of nanotube ropes that are trapped electrostatically are shown in Fig. 7. In Fig. 7(b) we observe a toroidal nanotube. This circular form of carbon nanotubes was discovered recently.²¹ Transport experiments on the nanotube ropes will be reported elsewhere.

The ET method was also tested on Pd colloid particles which were synthesized by Schmid and co-workers.²² These are almost identical Pd nanoparticles of about 20 nm in diameter. They are covered with a layer of stabilizing ligands of about 1 nm in thickness which prevent the coalescence of the particles. Due to the organic shell, the particles are soluble in water. Water has a finite conductivity, which in fact is much higher than the conductivity of a single Pd particle bridging the electrodes. This renders it impossible to observe trapping events directly in real time. Trapping can be achieved, however, in the following way. First we put on the electrodes a drop of water with dissolved Pd particles, then apply a voltage of 4.5 V to the electrodes through a series resistor of 100 M Ω which leads to a current of about 30 nA. After a few seconds the voltage is reduced to 0.45 V, and the water is removed with a flow of dry nitrogen gas. The resistance between the electrodes before the trapping

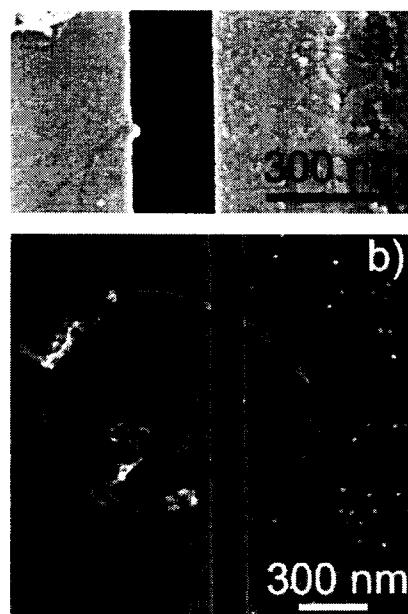


FIG. 7. (a) Bundle of nanotubes that has been trapped electrostatically between two AuPd electrodes separated by a slit of about 150 nm. (b) A toroidal nanotube (Ref. 21). The thicknesses of the ropes are about 6 and 25 nm, respectively.

procedure is very high (10^{13} Ω) and stays high after the drying if no particles were solved in the water, or if the voltage was not applied. Only if we use water with solved particles and apply a sufficiently high voltage, we observe a reduced resistance (a few G Ω) after the drying. Inspection with SEM shows that one or a few particles are trapped in the gap, depending on the distance between the electrodes. In Fig. 8 we present two examples.

Preliminary transport measurements show that the room temperature resistance of single Pd nanoparticles trapped between two electrodes has an exponential dependence on the bias voltage, i.e., $R \propto \exp(-V/V_0)$. The origin of this exponential behavior may tentatively be attributed to the voltage dependence of the tunnel barrier separating the particles from the electrodes. The barrier in this case is formed by the organic shell of the Pd particles. Tunneling through a monolayer of insulating organic molecules was studied by Boulas *et al.*,²³ who also observed an exponential drop of the resistance with increasing voltage. At 4 K we observe a gap in the current versus voltage characteristics indicating Coulomb blockade²⁴ effects. Details of the transport experiments will be reported elsewhere.

VI. CONCLUSIONS

We have demonstrated a technique of nanofabrication of electrodes separated by a gap of less than 5 nm. It is based on electron beam deposition of amorphous carbon and is carried out in a scanning electron microscope under direct visual control. Also we have suggested a new method of electrostatic trapping which provides a possibility to bridge the

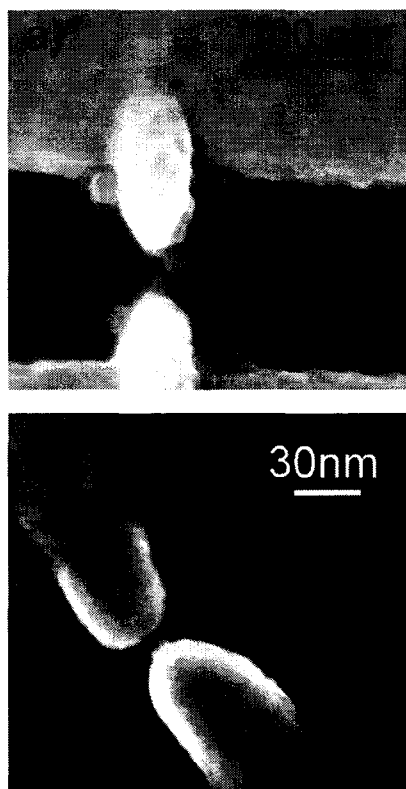


FIG. 8. Pd nanoparticles that are trapped electrostatically between electrodes. If the distance between the electrodes is smaller than the particle size then only a single particle is trapped as in (b). In the case of larger distances the electrodes are usually bridged with two or more particles as shown in (a). The metal films used for coating the electrodes were about 30 and 12 nm thick, respectively.

electrodes with a *single* conducting nanoparticle in a controlled way. This has been tested successfully for carbon nanotubes and Pd colloid particles. Transport measurements of single Pd colloid particles show an exponential dependence of the resistance on the applied voltage. Experiments on single conjugated molecules are in progress now.

ACKNOWLEDGMENTS

The authors are grateful to R. E. Smalley and G. Schmid for supplying carbon nanotubes and the Pd colloid, respectively. Interest and help of Y. Volokitin were important in the development of ET. Useful discussions with L. de Jongh, E. W. J. M. van der Drift, E. J. G. Goudena, P. M. Sarro, S. J. Tans, N. Gribov, and Y. Volokitin are acknowledged. This research was partly funded by the "Stichting voor Fundamenteel Onderzoek der Materie (FOM)."

¹A. Aviram and M. A. Ratner, Chem. Phys. Lett. **29**, 277 (1974); *Molecular Electronics—Science and Technology*, AIP Conf. Proc. 262, edited by A. Aviram (AIP, New York, 1992); *Introduction to Molecular Electronics*, edited by M. C. Petty, M. R. Bryce, and D. Bloor (Arnold, London, 1995).

²*Molecular Electronic Devices*, edited by F. L. Carter (Dekker, New York, 1982); L. Jones, D. L. Pearson, J. S. Schumm, and J. M. Tour, Pure Appl. Chem. **68**, 145 (1996).

³W. P. Su, J. R. Schrieffer, and A. J. Heeger, Phys. Rev. Lett. **42**, 1698 (1979); C. Joachim and J. F. Vinuesa, Europhys. Lett. **33**, 635 (1996); M. P. Samanta, W. Tian, and S. Datta, Phys. Rev. B **53**, 7626 (1996); V. Mujica, M. Kemp, and M. A. Ratner, J. Chem. Phys. **101**, 6849 (1994).

⁴A. N. Broers, IBM J. Res. Dev. **32**, 502 (1988).

⁵P. Bäuerle, T. Fischer, B. Bidlingmeier, A. Stabel, and J. P. Rabe, Angew. Chem. Int. Ed. Engl. **34**, 303 (1995); D. M. de Leeuw, Synth. Met. **55–57**, 3597 (1993).

⁶A. N. Broers, W. W. Molzen, J. J. Cuomo, and N. D. Wittels, Appl. Phys. Lett. **29**, 596 (1976).

⁷M. Wendel, H. Lorenz, and J. P. Kotthaus, Appl. Phys. Lett. **67**, 3732 (1995).

⁸Y. Akama, E. Nishimura, A. Sakai, and M. Murakami, J. Vac. Sci. Technol. A **8**, 429 (1990).

⁹D. L. Klein and P. L. McEuen, Appl. Phys. Lett. **68**, 1 (1996).

¹⁰V. Rousset, C. Joachim, S. Itoua, B. Rousset, and N. Fabre, J. Phys. III **5**, 1983 (1995).

¹¹M. A. Reed, C. Zhou, C. J. Muller, T. P. Burgin, and J. M. Tour (unpublished).

¹²H. W. van Zeijl, L. K. Nanver, and P. J. French, Electron. Lett. **31**, 927 (1995).

¹³L. A. Bumm, J. J. Arnold, M. T. Cygan, T. D. Dunbar, T. P. Burgin, L. Jones II, D. L. Allara, J. M. Tour, and P. S. Weiss, Science **271**, 1705 (1996).

¹⁴H. van Kempen, J. G. A. Dubois, J. W. Gerritsen, and G. Schmid, Physica B **204**, 51 (1995).

¹⁵A. Yu. Kasumov, I. I. Khodos, N. A. Kislov, O. V. Kononenko, V. N. Matveev, V. A. Tulin, Yu. B. Gorbakov, V. I. Nikolaichik, and E. E. Vdovin, Phys. Rev. Lett. **75**, 4286 (1995); V. V. Aristov, A. Yu. Kasumov, N. A. Kislov, O. V. Kononenko, V. N. Matveev, V. A. Tulin, I. I. Khodos, Yu. A. Gorbakov, and V. I. Nikolaichik, Nanotechnology **6**, 35 (1995).

¹⁶V. V. Aristov, N. A. Kislov, and I. I. Khodos, Microsc. Microanal. Microstruct. **3**, 313 (1992).

¹⁷C. E. Ells and G. D. Scott, J. Appl. Phys. **23**, 31 (1952); U. Oppenheim and J. H. Jaffe, *ibid.* **24**, 1521 (1953).

¹⁸H. W. Koops, A. Kaya, and M. Weber, J. Vac. Sci. Technol. B **13**, 2400 (1995); T. J. Stark, Y. M. Mayer, D. P. Griffis, and P. E. Russell *ibid.* **10**, 2685 (1992).

¹⁹S. Iijima, Nature (London) **354**, 56 (1991).

²⁰A. Thess, R. Lee, P. Nikolaev, H. Dai, P. Petit, J. Robert, C. Xu, Y. H. Lee, S. G. Kim, A. G. Rinzler, D. T. Colbert, G. E. Scuseria, D. Tomanek, J. E. Fischer, and R. E. Smalley, Science **273**, 483 (1996).

²¹J. Liu, H. Dai, J. H. Hafner, D. T. Colbert, R. E. Smalley, S. J. Tans, and C. Dekker Nature (London) **385**, 781 (1997).

²²G. Schmid, *Clusters and Colloids. From Theory to Applications* (VCH, Weinheim, 1994); *Physics and Chemistry of Metal Cluster Compounds*, edited by L. de Jongh (Kluwer, Dordrecht, 1994).

²³C. Boudas, J. V. Davidovits, F. Rondelez, and D. Vuillaume, Phys. Rev. Lett. **76**, 4797 (1996).

²⁴*Single-Charge Tunneling*, edited by H. Grabert and M. H. Devoret (Plenum, New York, 1992).